Advanced Materials Science

Research Article ISSN: 2398-6883

Construction of fusiform Co_3O_4 for supercapacitors

Changwei Lai[1#] and Weiwei Kang[2#*]

[1]Anyang Institute of Technology, Anyang, P R China.

[2]School of Chemistry and Chemical Engineering, Southeast University, PR China

[#]The authors contributed equally to this work

Abstract

A novel fusiform Co_3O_4 has been successfully synthesized by a solvothermal method. The fusiform structure can be synergistically determined by various characterization methods (such as XRD, XPS, SEM and TEM). Owing to the special morphology of fusiform Co_3O_4, it achieves specific capacitances of 544.3 F g^{-1} at the current densities of 0.5 A g^{-1} in a three-electrode system, exhibiting excellent cycling stability with a specific capacitance retention of 81.9% after 2000 cycles at a current density of 20 A g^{-1}.

Introduction

Supercapacitors (SCs) have drawn great extensive attention in the past few decades because they have an ultrafast charge and discharge rate, good reliability, high power density and long cycling performance [1-3]. SCs can be generally classified into three types based on their energy storage mechanism: electrical double-layer capacitors (EDLCs) [4], pseudocapacitors [5] and hybrid supercapacitors [6,7]. Pseudocapacitors are governed by fast and reversible Faradaic redox reactions at the effective near-surfaces of the electrode materials. Transition metal oxides (TMOs) are recognized as ideal pseudocapacitive materials due to the enhanced capacitance and higher energy density than those of EDLCs [8,9]. Among the TMOs, RuO_2 has been considered as the most promising Faradaic pseudocapacitors materials [10,11]. However, RuO_2 is restricted in practical application because of its low porosity, toxic nature, and high cost. In view of the facts, Co_3O_4 attracts extensive interest for pseudocapacitor electrode materials due to its extremely high theoretical capacitance of 3560 F g^{-1}, high redox activity, good electrochemical performance, high natural abundance, low cost, and environmental friendliness [12,13]. Up to now, many available methodologies have been developed to achieve various special Co_3O_4 nanostructures for supercapacitors [14-16].

Herein, we have prepared the fusiform Co_3O_4 for pseudocapacitors electrode materials, and further study the electrochemical properties of the fusiform Co_3O_4 in a three electrode configuration.

Experimental

Preparation of the fusiform Co_3O_4

4.8 mmol of $Co(NO_3)_2 \cdot 6H_2O$ and 0.8 mL of deionized water were dissolved in 30 mL of methanol under magnetic stirring, then 1.5 g of sodium dodecylbenzenesulfonate (SDBS) was added into the reaction solution, and the mixture was sonicated for 1 h to form a blue colloidal suspension. The resulting mixture was transferred into 40 mL Teflon-lined stainless steel autoclave liners and maintained at 200°C for 4 h. After cooling to room temperature naturally, the precipitates were filtered and washed with deionized water, then dried under vacuum oven at 60°C for 12 h. Finally, the samples were sintered in a muffle furnace in air to obtain the Co_3O_4 at 35°C for 2 h.

Characterization

The structures of products was analyzed by X-ray diffraction (XRD) on a D8-Discover diffractometer (Bruker, Germany) with Cu Ka radiation (λ= 0.154 nm). Detailed elemental analysis was carried out with an ESCALAB-250 X-ray photoelectron spectroscopy (XPS) (ThermoFisher Scientific, USA). Thermogravimetric analysis (TGA) was carried out on a SDT-Q600 instrument. The morphology of materials was identified by scanning electron microscopy (SEM, HITACHI S-4800) and transmission electron microscopy (TEM, Philips Tecnai-12).

Electrochemical measurements

In the three-electrode system, the CV tests of individual electrodes were carried out in the potential range of -0.2 - 0.6 V vs. saturated calomel reference electrode (SCE) by varying the scan rate from 2 to 100 mV s^{-1}. GCD was performed at different current densities varying from 0.5 to 40 A g^{-1}. The specific capacitance (C, F g^{-1}) of the electrode was calculated by using the following equations: $C = (I\,\Delta t)/(m\,\Delta V)$, where C is the specific capacitance (F g^{-1}), I is the discharge current (A), Δt is the total discharge time (s), m is the mass (g) of the active material in the electrode and ΔV is the potential range in the discharge process (V), respectively.

Results and discussion

Characterization of the structure

The crystalline structure of Co_3O_4 was confirmed by X-ray diffraction (XRD). Figure 1a shows the XRD patterns of Co_3O_4, exhibiting diffraction peaks attribute to the (111), (220), (311), (222),

Correspondence to: Weiwei Kang, School of Chemistry and Chemical Engineering, Southeast University, Nanjing, 211189, PR China, E-mail: weiweikangwell@163.com

Key words: *fusiform, Co3O4, supercapacitors*

Received: July 27, 2018; **Accepted:** August 27, 2018; **Published:** August 30, 2018

(400), (422), (511) and (440) planes of the cubic Co_3O_4 phase (JCPDS 42-1467), respectively. These features suggest that the as-prepared materials are crystallized well. To further ditermine the Co_3O_4 structure, the Co 2p XPS spectrum indicates that two main peaks at 781.1 and 796.1 eV, corresponding to the Co $2p_{3/2}$ and Co $2p_{1/2}$ with a spin-orbit splitting of 15.0 eV as shown in the figure 1b [17]. And it can further verify the formation of Co_3O_4 by the two prominent shake-up satellite peaks (denoted as "Sat.") for Co^{2+}, which is consistent with the observation from XRD. In the low and high-magnification SEM images (Figure 1c), the fusiform Co_3O_4 shows average short diameter of 10-12 μm and the both ends in a range of 20-25 μm. Moreover, the transmission electron morphology (TEM) image can further confirm the fusiform morphology (Figure 1d).

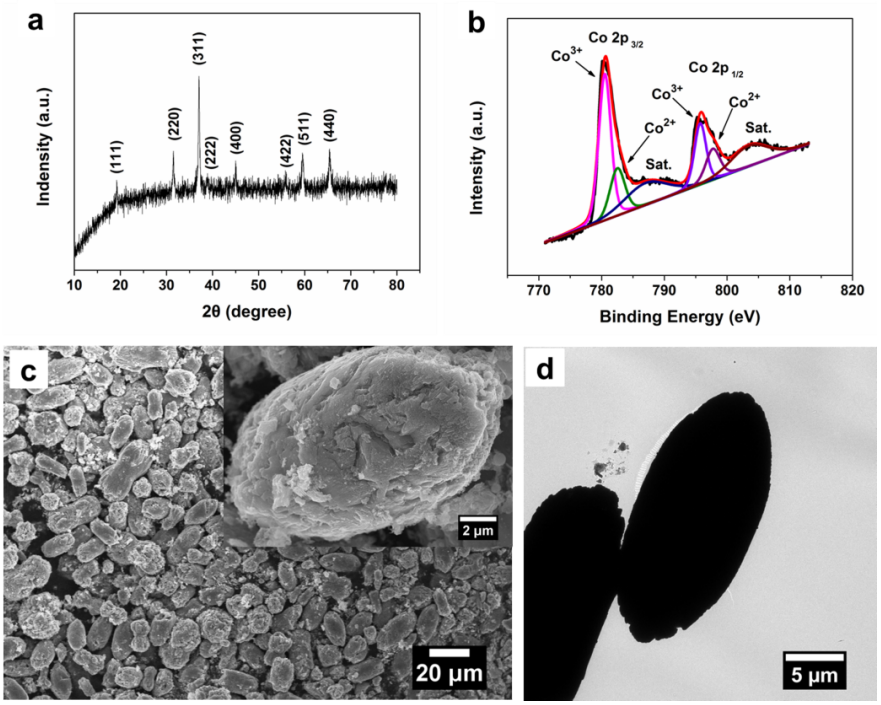

Figure 1. (a) XRD pattern, (b) Co 2p XPS spectrum, (c) Low and high-magnification (inset) SEM images, (d) TEM image of the fusiform Co_3O_4

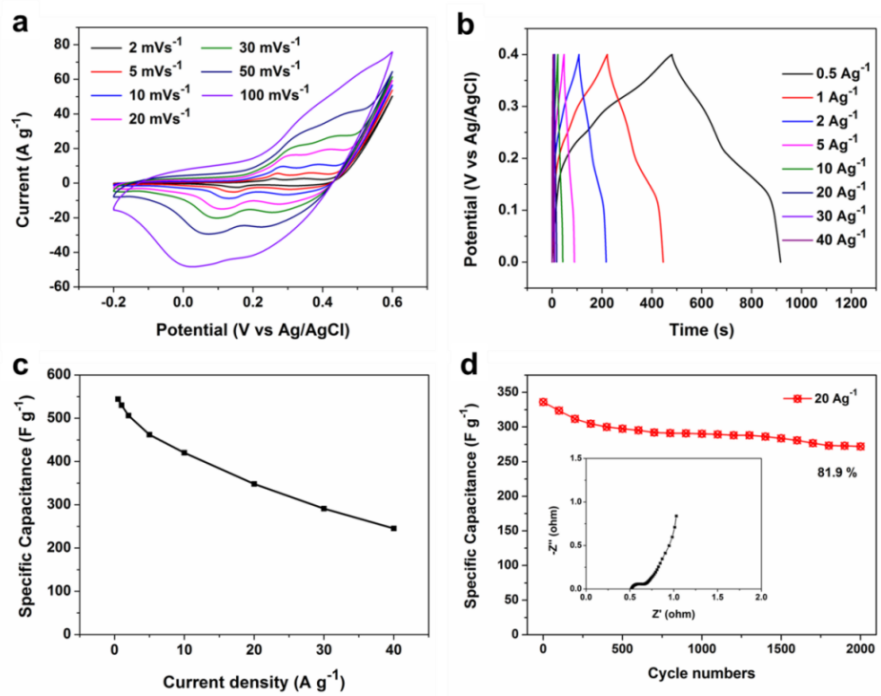

Figure 2. The electrochemical properties of Co_3O_4: (a) CV curves at different scan rates. (b) Galvanostatic charge-discharge curves at different current densities. (c) The specific capacitance at various current densities. (d) Cycling performance at a current density of 20 A g^{-1} (the inset shows the Nyquist plots)

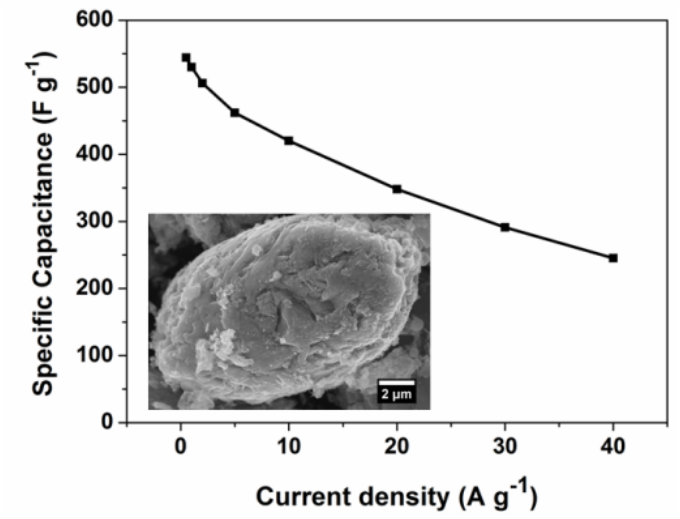

Figure 3. A novel fusiform Co_3O_4 exhibits an excellent pseudocapacitive performance

Electrochemical properties

The electrochemical properties of the fusiform Co_3O_4 were systematically studied by cyclic voltammograms (CV) and galvanostatic charge-discharge (CD) in three electrode configuration. In figure 2a, the CV curves of Co_3O_4 show the obvious pseudocapacitance features in 6 M KOH solution. The redox peaks in CV curves can be ascribed to the conversions between different cobalt oxidation states, according to the follow sequential reactions [18,19]:

$$Co_3O_4 + OH^- + H_2O \leftrightarrow 3CoOOH + e^- \quad (1)$$

$$CoOOH + OH^- \leftrightarrow CoO_2 + H_2O + e^- \quad (2)$$

Figure 2b shows the CD curves of the fusiform Co_3O_4 at different current densities from 0.5 to 40 A g^{-1}. A higher specific capacitance value of 544.3 F g^{-1} at a current density of 0.5 A g^{-1} was achieved (Figure 2c). Moreover, the long-term stability of Co_3O_4 was carried out using the charge-discharge cycling test at a high current density of 20 A g^{-1}. After 2000 cycles, it retains 81.9 % of its initial capacitance (Figure 2d). From the EIS spectra of the fusiform Co_3O_4 (inset), the electrochemical resistance (R_s) and charge transfer resistance (R_{ct}) are respectively determined as around 0.53 Ω and 0.62 Ω, demonstrating the electrical conductivity and ion transfer of the as-prepared materials (Figure 3).

Conclusion

In summary, we demonstrate a novel fusiform Co_3O_4, exhibiting an excellent pseudocapacitive performance. It is believed that this study may open up a new research strategy for Co_3O_4 has a potential promising performance for pseudocapacitors electrode materials.

Acknowledgements

This work was supported by the National Natural Science Foundation of China (no. 21304018, 51404098, 51174077).

References

1. Chen H, Zhou M, Wang T, Li F, Zhang YX (2016) Construction of unique cupric oxide–manganese dioxide core–shell arrays on a copper grid for high-performance supercapacitors. *J Mater Chem A* 4: 10786-1079.
2. Zhao RR, Li K, Liu RZ, Sarfraz M, Shakir I, et al. (2017) Reversible 3D self-assembly of graphene oxide and stimuli-responsive polymers for high-performance graphene-based supercapacitors. *J Mater Chem A* 5: 19098-19106.
3. Li K, Huang YS, Liu JJ, Sarfraz M, Agboola PO, et al. (2018) A three-dimensional graphene framework-enabled high-performance stretchable asymmetric supercapacitor. *J Mater Chem A* 6: 1802-1808.
4. Xu Y, Sheng K, Li C, Shi G (2010) Self-assembled graphene hydrogel via a one-step hydrothermal process. *ACS Nano* 4: 4324-4330. [Crossref]
5. Wang H, Xu C, Chen Y, Wang Y (2017) MnO_2 nanograsses on porous carbon cloth for flexible solid-state asymmetric supercapacitors with high energy density. *Energy Storage Mater* 8: 127-133.
6. Miniach E, Śliwak A, Moyseowicz A, Fernández-Garcia L, González Z, et al. (2017) MnO_2/thermally reduced graphene oxide composites for high-voltage asymmetric supercapacitors. *Electrochim Acta* 240: 53-62.
7. Zeng X, Yang B, Li X, Yu R (2017) Three-dimensional hollow CoS_2 nanoframes fabricated by anion replacement and their enhanced pseudocapacitive performances. *Electrochim Acta* 240: 341-349.
8. Hong J, Lee YW, Ahn D, Pak S, Lee J, et al. (2017) Highly stable 3D porous heterostructures with hierarchically-coordinated octahedral transition metals for enhanced performance supercapacitors. *Nano Energy* 39: 337-345.
9. Wen Y, Rufford TE, Chen X, Li N, Lyu M, et al. (2017) Nitrogen-doped Ti_3C_2Tx MXene electrodes for high-performance supercapacitors. *Nano Energy* 38: 368-376.
10. Kim H, Popov BN (2002) Characterization of hydrous ruthenium oxide/carbon nanocomposite supercapacitors prepared by a colloidal method. *J Power Sources* 104: 52-61.
11. Chen LY, Hou Y, Kang JL, Hirata A, Fujita T, et al. (2013) Toward the theoretical capacitance of RuO_2 reinforced by highly conductive nanoporous gold. *Chen Adv Energy Materials* 3: 851-856.
12. Liao Q, Li N, Jin S, Yang G, Wang C (2015) All-Solid-State Symmetric Supercapacitor Based on Co_3O_4 Nanoparticles on Vertically Aligned Graphene. *ACS Nano* 9: 5310-5317. [Crossref]
13. Zheng Y, Li Z, Xu J, Wang T, Liu X, et al. (2016) Multi-channeled hierarchical porous carbon incorporated Co_3O_4 nanopillar arrays as 3D binder-free electrode for high performance supercapacitors. *Nano Energy* 20: 94-107.
14. Jiang J, Shi W, Song S, Hao Q, Fan W, et al. (2014) Solvothermal synthesis and electrochemical performance in super-capacitors of Co_3O_4/C flower-like nanostructures. *J Power Sources* 248: 1281-1289.
15. Wang H, Zhang L, Tan X, Holt CM, Zahiri B, et al. (2011) Supercapacitive properties of hydrothermally synthesized Co_3O_4 nanostructures. *J Phys Chem C* 115: 17599-17605.
16. Liao Q, Li N, Jin S, Yang G, Wang C (2015) All-Solid-State Symmetric Supercapacitor Based on Co_3O_4 Nanoparticles on Vertically Aligned Graphene. *ACS Nano* 9: 5310-5317. [Crossref]
17. Wang R, Xu C, Sun J, Liu Y, Gao L, et al. (2013) Free-standing and binder-free lithium-ion electrodes based on robust layered assembly of graphene and Co_3O_4 nanosheets. *Nanoscale* 5: 6960-6967. [Crossref]
18. Liao Q, Li N, Jin S, Yang G, Wang C (2015) All-Solid-State Symmetric Supercapacitor Based on Co_3O_4 Nanoparticles on Vertically Aligned Graphene. *ACS Nano* 9: 5310-5317. [Crossref]
19. Rakhi RB, Chen W, Cha D, Alshareef HN (2012) Substrate dependent self-organization of mesoporous cobalt oxide nanowires with remarkable pseudocapacitance. *Nano Lett* 12: 2559-2567. [Crossref]